THE ASTROPHYSICAL JOURNAL, 499:000–000, 1998 June 1
© 1998. The American Astronomical Society. All rights reserved. Printed in U.S.A.

DISCOVERY OF AN ULTRAFAST X-RAY PULSAR IN THE SUPERNOVA REMNANT N157B

F. E. MARSHALL,[1] E. V GOTTHELF,[1,2] W. ZHANG,[1] J. MIDDLEDITCH,[3] AND Q. D. WANG[4]

Received 1998 March 4; accepted 1998 April 6; published 1998 May 8

ABSTRACT

We present the serendipitous discovery of 16 ms pulsed X-ray emission from the Crab-like supernova remnant N157B in the Large Magellanic Cloud. This is the fastest spinning pulsar associated with a supernova remnant (SNR). Observations with the *Rossi X-Ray Timing Explorer* (*RXTE*), centered on the field containing SN 1987A, reveal an X-ray pulsar with a narrow pulse profile. The archival *Advanced Satellite for Cosmology and Astrophysics* (*ASCA*) X-ray data confirm this detection and locate the pulsar within 1′ of the supernova remnant N157B, 14′ from SN 1987A. The pulsar shows evidence of glitch(es) between the 3.5 yr separating the *RXTE* and *ASCA* observations; the mean linear spin-down rate is $\dot{P} = 5.126 \times 10^{-14}$ s s^{-1}. The background-subtracted, pulsed emission is similar to other Crab-like pulsars with a power law of photon index ~1.6. The characteristic spin-down age (~5000 yr) is consistent with the previous age estimate of the SNR. The inferred *B*-field for a rotationally powered pulsar is $\sim 1 \times 10^{12}$ G. Our result confirms the Crab-like nature of N157B ; the pulsar is likely associated with a compact X-ray source revealed by *ROSAT* HRI observations.

Subject headings: pulsars: general — pulsars: individual (PSR J0537−6910) — supernova remnants — X-rays: general

1. INTRODUCTION

Crab-like supernova remnants (SNRs) play a critical role in our understanding of young pulsars and their pulsar wind nebulae. These rare SNRs that contain central pulsars are distinguished by their centrally filled morphologies and nonthermal X-ray spectra. The X-ray emission of such SNRs comes predominantly from a synchrotron nebula powered by an embedded young pulsar (e.g., Seward 1989). Only three confirmed members of this class were previously known: the Crab Nebula, with its famous 33 ms pulsar PSR B0531+21, the SNR B0540−693 in the Large Magellanic Cloud (LMC), with its 50 ms pulsar PSR B0540−69, and the nebula around the 150 ms pulsar PSR B1509−58. Several candidate Crab-like SNRs have been reported. These have similar morphologies and spectral characteristics but so far lack a detected pulsar. Young Crab-like SNRs are expected to evolve into composite SNRs, in which the thermal emission from shock-heated gas will rival or exceed the diminishing X-ray radiation from the pulsar-powered synchrotron nebulae. This evolutionary sequence is not yet firmly established, though, mainly because of the limited number of samples.

We report in this Letter the discovery of an ultrafast pulsar in N157B (also known as NGC 2060, SNR 0538−69.1, and 30 Doradus B; Henize 1956), confirming the Crab-like nature of this remnant (Wang & Gotthelf 1998 and references therein). The pulsar was first detected serendipitously with *Rossi X-Ray Timing Explorer* (*RXTE*) data while searching for a pulsed signal from nearby SN 1987A. We used archival *Advanced Satellite for Cosmology and Astrophysics* (*ASCA*) data of the region to confirm the detection of the pulsed emission, to measure its spin-down rate, and to locate the emission to within the boundary of N157B. Based on the *ASCA* position, we will refer to the pulsar as PSR J0537−6910. In the following, we present our discovery of PSR J0537−6910 and discuss its properties in the context of other young pulsars.

[1] Laboratory for High Energy Astrophysics, NASA/GSFC, Greenbelt, MD 20771; frank.marshall@gsfc.nasa.gov, gotthelf@gsfc.nasa.gov, zhang@xancus10.gsfc.nasa.gov.

[2] Universities Space Research Association.

[3] Los Alamos National Laboratory, P.O. Box 1663, MS B256, CIC-19, Los Alamos, NM 87545; jon@lanl.gov.

[4] Dearborn Observatory, Northwestern University, 2131 Sheridan Road, Evanston, IL 60208-2900; wqd@nwu.edu.

2. OBSERVATIONS

The LMC field containing SN 1987A has been sampled frequently by many X-ray observatories, including *RXTE* and *ASCA*. There were two observing runs in 1996 with *RXTE* to search for pulsations from SN 1987A (see the observation log, Table 1). The first was an uninterrupted observation of 21 ks on 1996 October 12. The other run, which began on 1996 December 20, obtained a total of about 78 ks of good observing time during an elapsed time of 184 ks.

The *RXTE* Observatory (Bradt, Rothschild, & Swank 1993) consists of five co-aligned collimated detectors known collectively as the Proportional Counter Array (PCA), a set of crystal scintillation detectors known as the High Energy X-ray Timing Experiment, and the All-Sky Monitor. Here we report exclusively on data obtained with the PCA because of its large effective area (~6500 cm^2 at 10 keV). The PCA (Jahoda et al. 1996) has collimators that produce a roughly circular aperture with a ~1° FWHM response. There are several known X-ray sources within the field of view (FOV) with flux above 2 keV, the brightest of which are the black hole candidate LMC X-1, the 50 ms pulsar PSR B0540−69, and N157B, the object of this study. The PCA observations used the Good Xenon data mode, which time tags each photon with 0.9 μs timing resolution. For the current analysis, the absolute timing uncertainty is ~100 μs (Rots et al. 1998). Moderate spectral information is available in the 2–60 keV energy band with a resolution of ~16% at 6 keV.

The *ASCA* Observatory (Tanaka, Inoue, & Holt 1994) acquired three long ~20 ks observations of the region around SN 1987A with sufficient timing resolution to detect millisecond pulsations (see Table 1). These were all obtained in 1993 during the early Performance and Verification phase of the *ASCA* mission. Two of the observations containing N157B were optimal, placing the SNR close to the optical axis, while the third data set observed the SNR with reduced efficiency, at 18′ off-axis where the source flux is strongly vignetted.

TABLE 1
OBSERVATION LOG FOR PSR J0537−6910

Data Set	Date[a] (UT)	Epoch[a] (MJD)	Exposure/Duration (ks)	Period (ms)	Uncertainty (ns)	Pulsed Flux[b] ($\times 10^{-13}$ ergs s^{-1} cm^{-2})
ASCA	1993 Jun 13	49151.306618	30.8/89.4	16.1093291	0.15	6.4 ± 0.8
	1993 Aug 20	49219.986830	32.1/94.8	16.1096349	0.11	7.1 ± 0.9
	1993 Sep 23	49253.982891	35.6/82.8	16.1097864	0.15	4.1 ± 2.0
RXTE	1996 Oct 12	50368.148905	21.8/21.8	16.1147174	0.30	6.8 ± 1.2
	1996 Dec 20	50437.550201	78.0/184.5	16.11502765	0.03	6.7 ± 0.7

[a] Start of the observation.
[b] The unabsorbed pulsed *RXTE* and *ASCA* flux using an absorbed power-law model of photon index 1.6, in the 2–10 keV energy band. The *ASCA* GIS flux is derived using photons extracted from a 4′ radius aperture centered on the *ASCA* N157B position. The off-pulse spectrum was used as a background (see text for details).

ASCA data were acquired with all four co-aligned focal-plane instruments. We used data exclusively from the two Gas Imaging Spectrometers (GISs) and only data for which time-tagged photons were available in the highest time resolution mode (61 μs or 0.488 ms, depending on telemetry rate). *ASCA* GIS timing measurements are found to have an absolute accuracy of 200 μs in this mode (see Saito et al. 1997). Data from the Solid-State Imaging Spectrometers do not have adequate time resolution for the current study. The GIS offers ~8% spectral resolution at 6 keV over its ~1–12 keV energy bandpass. Each GIS sits at the focus of a conical foil mirror, and the combination results in a spatial resolution of 1′–3′ (depending on energy) over the GIS's ~50′ diameter active FOV. Point sources can be located with ~0.′6 accuracy (see Gotthelf 1994).

Both the *RXTE* and *ASCA* data were edited to exclude times of high background contamination using the standard processing screening criteria ("REV2" for *ASCA*). This rejects time intervals of South Atlantic Anomaly passages, Earth occultations, the bright Earth limb in the field of view (*ASCA* only), and other periods of high particle activity. For each observation, event data from all detectors were co-added and the arrival times of each photon corrected to the solar system barycenter using the JPL DE200 ephemeris.

3. TIMING RESULTS

In this Letter, we have concentrated on *RXTE* data collected in the 2–10 keV energy band in layer 1 of the PCA, which provides the best sensitivity for weak sources with a Crab-like spectrum, and the ~8–25 keV hard energy band using all three PCA layers. We also examined data above 30 keV, which are expected to be dominated by detector background, to verify that there are no similar periodicities produced by the instrument itself.

We searched for possible periodic signals using fast Fourier transforms of the data binned in 0.16 ms steps. The 1996 October 12 observation produced a 7.5 σ signal at ~62.055 Hz in the hard energy band, including power from the second and third harmonics. The probability of false detection is less than 1 in 10^{10}. This result is reproduced in the 2–10 keV band data, with a 10 σ detection in the first three harmonics of the 62 Hz signal. No other significant power was found, with the exception of frequencies corresponding to the 50 ms pulsar PSR B0540−69. The new frequencies are not simple harmonics or aliases of the 50 ms pulsar signal. As we show below, any association with the 50 ms pulsations can be ruled out conclusively. We folded the data into 20 bins on periods near 16 ms and computed χ^2 for a model with a count rate independent of pulse phase. The largest value for χ^2 of 157 (10 σ) was found for a period of $P = 16.114717$ ms. The pulsar was also detected during the second *RXTE* observing run, allowing us to derive an initial period derivative.

We examined the *ASCA* data for the *RXTE* pulsations. N157B was considered the most likely source of the pulsations because it is the brightest source in the *RXTE* FOV after LMC X-1 and B0540−693. It is a barely resolved, moderately bright *ASCA* source in the 30 Doradus star formation region. N157B is clearly imaged in the *ASCA* GIS as an isolated source, ~10′ southwest of the X-ray–bright R136 region and ~15′ northwest of the 50 ms pulsar PSR B0540−69, which produced stray light in the *ASCA* FOV containing N157B.

We constructed a periodogram of the *ASCA* GIS data using photons extracted from a 4′ radius aperture centered on the peak flux from N157B. For each trial period, we folded the data into 10 bins to optimize the signal in the photon noise–dominated data and computed the χ^2 of the resultant profile. From each *ASCA* observation, we conducted a high-resolution blind search of the data for significant power about a range of ± 0.5 ms around the expected period. To search for short duty cycle pulsations in period-space, we oversampled the period resolution by a factor of 20, using increments of $0.05\ (P^2/T)$, where T is the observation duration and P is the test period.

A highly significant signal (>12 σ) was found during both on-axis *ASCA* observations. The low signal-to-noise ratio, 1993 September observation produced a 5 σ result, whose reduced significance is consistent with the target being placed 18′ off-axis. This is the only significant peak found from all data sets, over the range searched. We used the change in the period between the two on-axis observations to bootstrap the period derivative, which resulted in a search of greater sensitivity. We also find that the period detection is greatly improved by excluding photons below less than 2 keV. This suggests that the pulsar signal is significantly contaminated by unpulsed, soft thermal flux from the SNR nebula, which dominates below 2 keV. The nondetection of the pulsar by Wang & Gotthelf (1998) is explained by the narrowness of the peak, the duration of the observations (typically 90 ks), and the lack of a period derivative a priori.

Since it is not possible to maintain phase between any of the four observation intervals, estimates of the period derivative are based on the change in period between observations. Figure 1 shows the period evolution and the residuals from the best-fit linear model of $P = 0.016113089$ s ± 1.7 ns at MJD 50,000 (at Earth) and $\dot{P} = 5.126 \pm 0.002 \times 10^{-14}$ s s^{-1}. Our estimates of the period uncertainty for each data point in Figure 1 are derived by Monte Carlo simulation and maximum likelihood analysis. Clearly, there are significant deviations from a constant period derivative; these are not removed by including a period second derivative to the fit. This inability to find a

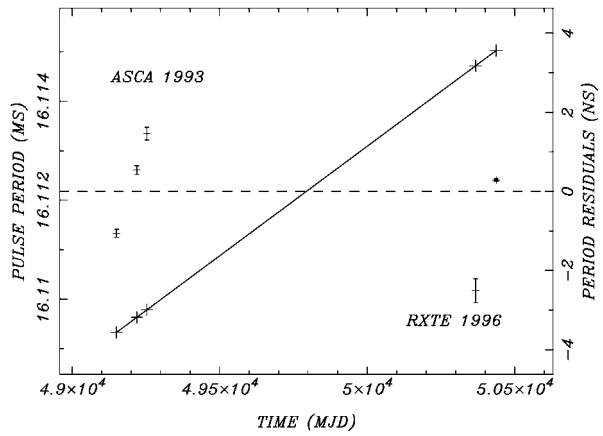

FIG. 1.—The pulse period evolution of PSR J0537−6910 and its residuals from the best-fit model (*solid line*) assuming a linear spin-down trend (see text). The period measurements are marked by the crosses along the line; the error bars are smaller than the width of the line on this scale (*left ordinate*). The period residuals using this model are denoted by the points with error bars (*right ordinate*).

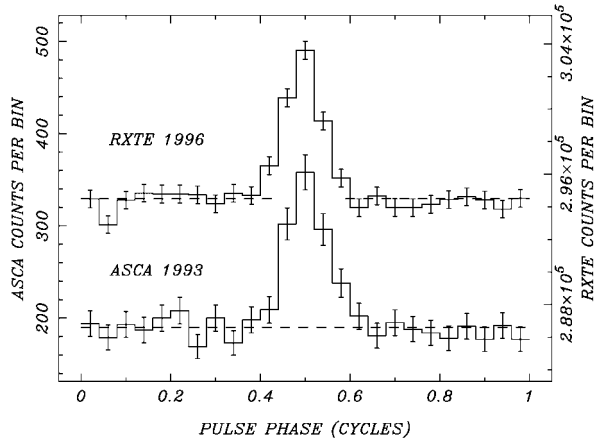

FIG. 2.—The pulse profile of PSR J0537−6910 in the 2–10 keV band from the *RXTE* (*top*) and *ASCA* (*bottom*) observations. The two profiles have been aligned to place the peak emissions at the 0.5 phase bin. The relative phases of the two measurements are arbitrary. The *RXTE* profile includes 100 ks of data; the *ASCA* profile is restricted to the 37 ks of 64 μs resolution data.

single solution for both sets of observations suggests that one or more glitches in the period have occurred (see discussion in § 4). The measured period derivatives during the two epochs are $\dot{P}_{ASCA} = 5.154 \pm 0.002 \times 10^{-14}$ s s^{-1} and $\dot{P}_{RXTE} = 5.174 \pm 0.002 \times 10^{-14}$ s s^{-1}.

Using the above ephemerides, we generated pulse profiles for the 1993 *ASCA* and the 1996 *RXTE* combined data sets. The resulting profiles are displayed in Figure 2. They are well characterized by a single, narrow-peaked pulse with an approximately Gaussian shape of FWHM of ~1.7 ms (10% duty cycle). The profiles appear unchanged between the 1993 and 1996 observations. The pulsed emission comprises 9.6% of the total *ASCA* counts in the 4′ radius aperture above 2 keV.

To demonstrate that these pulsations are uniquely associated with N157B, an image of the pulsed emission was generated by subtracting the off-pulsed data from the on-pulsed image. Only a single source of significant emission remained, the pulsed emission, an unresolved *ASCA* pointlike source located at the coordinates of the SNR N157B (see Wang & Gotthelf 1998). We thus reproduce and verify the *RXTE* measurement and unambiguously locate the origin of the pulsed emission to within the ~1′ region encompassing N157B.

In summary, we consider this a conclusive detection of a new pulsar in N157B, PSR J0537−6910, whose period of 16 ms makes it the fastest known pulsar associated with an SNR.

4. DISCUSSION

The steady increase in the period suggests that the pulsed X-ray emission is powered by the spin-down energy loss of the pulsar. We estimate the spin-down power as $\dot{E} = (2\pi)^2 I\dot{P}/P^3 = 4.8 \times 10^{38} I_{45}$ ergs s^{-1}, where I_{45} is the moment of inertia of the neutron star in units of 10^{45} g cm^2. For a pulsar losing rotational energy via magnetic dipole radiation, $\dot{E} \sim (B_p^2 R^6 \Omega^4)/(6c^3)$, and the surface magnetic field strength at the pole is $B_p \sim 1 \times 10^{12}$ G. Here $R \sim 10$ km is the neutron star radius, $\Omega = 2\pi/P$ is the angular velocity of the rotation, and c is the speed of light.

The pulsed spectral component can be isolated using phase-resolved spectroscopy. The source photons were folded at the best-measured period, and phase-dependent spectra constructed. Using the off-pulse spectrum as background, we fitted the on-pulse spectrum with a simple absorbed power-law model to the *ASCA* and *RXTE* data in the 2–20 keV band. The best-fit photon index ($\chi_\nu^2 = 0.96$ for 30 degrees of freedom) is 1.6 (1.3–2.0), which is consistent with the typical value of ~1.7 for other pulsars (Lyne & Graham-Smith 1990). The large uncertainties are due to subtracting two spectra with a similar number of counts. The unabsorbed 2–10 keV pulsed flux of PSR J0537−6910 is ~$(6.7 \pm 0.6) \times 10^{-13}$ ergs s^{-1} cm^{-2} (see Table 1). The corresponding pulsed luminosity is ~1.7×10^{35} ergs s^{-1} (into 4π), assuming a distance of 47 kpc (Gould 1995).

The derived pulsed luminosity suggests that ~4×10^{-4} of the pulsar's spin-down energy is emitted as pulsed X-rays in the 2–10 keV band. This luminosity is consistent with the empirical relation, $L_X \approx 7 \times 10^{26} (B_{12}/P_s^2)^{2.7}$ ergs s^{-1}, which fits well to the magnetorotation-driven X-ray emission from previously known pulsars (Ögelman 1995). Here B_{12} is the magnetic field in units of 10^{12} G, and P_s^2 is the spin period in units of seconds.

Compared with other young pulsars known to be associated with Crab-like SNRs, PSR J0537−6910 is quite unusual. Its X-ray pulse profile appears to be the narrowest among the young pulsars. The Crab pulsar is double-peaked, and the profiles of both PSR B0540−69 and PSR B1509−58 are very broad (duty cycle >0.3). The pulse width of PSR J0537−6910, 1.7 ms, indicates that the size of the emission region is likely smaller than about half of the light cylinder radius. A detailed study of the pulse profile may help constrain pulsar emission models. The characteristic age of the pulsar is $\tau = P/(2\dot{P}) = 5 \times 10^3$ yr. This age is much greater than any of the other Crab-like pulsars, yet similar to the age estimate for N157B of ~5×10^3 yr, based on X-ray measurements of the size and temperature of the remnant (Wang & Gotthelf 1998). An upper limit on the age of the remnant, based on the kinematics of Hα-emitting gas in the region (Chu et al. 1992), suggests that the remnant may be as old as ~2×10^4 yr.

An accurate determination of the remnant age is critical for estimating the initial rotation rate of the pulsar. PSR J0537−6910 rotates twice as fast as the Crab pulsar and was likely spinning much more rapidly when it was born, depending on its assumed braking index and age. Following Kaspi et al. (1997), we plot in Figure 3 the possible initial spin period

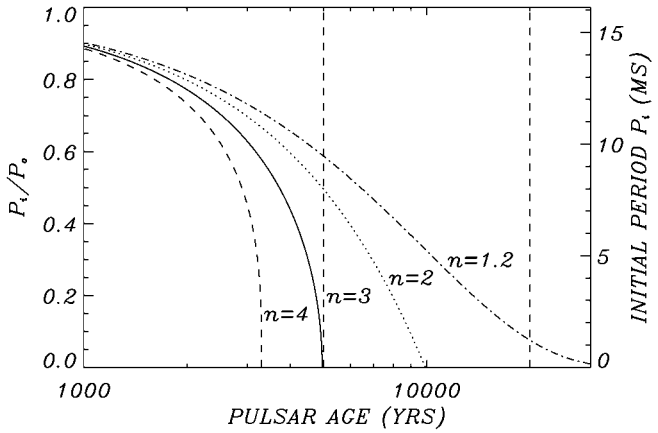

FIG. 3.—Predicted initial period of PSR J0537−6910 as a function of the age of the pulsar. Here we have assumed a power-law deceleration model $P \propto P^{2-n}$ (e.g., Shapiro & Teukolsky 1983). The four curves corresponds to different values of the index: 1.2 (*dot-dashed*), 2 (*dotted*), 3 (*solid*), and 4 (*dashed*). The vertical lines indicate a pulsar age of 5×10^3 and 20×10^3 yr old.

versus age for a range of braking indices. If the older age estimate is correct and if glitches are not important in the overall period evolution of the pulsar, the braking index would then have to be unusually small ($\leq$1.2) for an initial period $\geq$1 ms. If the younger value for the age is more likely, the initial spin is then a few milliseconds, assuming $n \sim 3$, as in the case of the magnetic dipole model and for other young pulsars. In either case, these values provide important constraints on neutron star birth spin models.

The phenomena of pulsar glitches are well established and provide important constraints on the moment of inertia of neutron stars (see Shapiro & Teukolsky 1983, chap. 10, p. 267). These sudden changes in the pulsar spin period and period derivative are attributed to "starquakes," stress relief between the neutron star crust and the superfluid core. Monitoring of the Crab and Vela pulsars, as well as other young pulsars, shows that large glitches occur on timescales of a few years. There is compelling evidence that PSR J0537−6910 has undergone one or more glitches between the *ASCA* and *RXTE* epochs (see Fig. 1). The integrated magnitude of the glitches, $\Delta\Omega/\Omega \sim 10^{-6}$, is comparable to that observed from the Vela pulsar, but substantially larger than any of those observed from the Crab pulsar. More careful analysis of the data is still needed, however, to quantify the presence of any glitches and to distinguish them from timing noise.

The origin of the unpulsed X-rays detected from N157B in the energy band $\geq$2 keV is likely a synchrotron nebula powered by the pulsar via a relativistic wind (Gallant & Arons 1994 and references therein). Recent work by Wang & Gotthelf (1998) has shown that N157B contains a bright, elongated, and nonthermal X-ray feature whose origin is still uncertain. Attached to this feature is a compact source with a spatial extent of ~7″, which they claim most likely represents the pulsar and its interaction with the surrounding medium. The X-ray spectrum of N157B, which is dominated by the unpulsed emission, can be characterized by a power law with an energy slope ~1.5 (Wang & Gotthelf 1998), significantly steeper than those (~1.0) of other Crab-like SNRs (e.g., Asaoka & Koyama 1990). The remnant has probably evolved to a stage close to that of a composite SNR. This steep spectrum and the elongated morphology suggest that something unusual may be happening in N157B. Most likely, relativistic particles are transported from the pulsar to a radio-emitting wind bubble in a collimated outflow (Wang & Gotthelf 1998); a substantial fraction of high-energy particles from the pulsar lose their energy radiatively in a bow shock, rather than adiabatically through diffusion.

5. CONCLUSION

We have found 16 ms pulsed X-ray emission from the 30 Doradus region of the LMC. We have shown that these pulsations are associated uniquely with the X-ray emission from the SNR N157B. This remnant is an important new addition to the class of Crab-like SNRs. It provides a rare laboratory for studying both an unusually rapidly rotating pulsar and its relativistic wind, as well as the structure and evolution of a neutron star. Future observations are important to constrain the age of the pulsar, the period second derivative, and to measure putative glitches.

We thank the *RXTE* and *ASCA* teams for making these observations possible. We thank V. Kaspi for discussions and a careful reading of the manuscript. This research made use of data obtained through the HEASARC on-line service, provided by NASA/GSFC. E. V. G. is supported by USRA under NASA contract NAS5-32490. Q. D. W. is supported partly by NASA LTSA grant NAG5-6413.

REFERENCES

Asaoka, I., & Koyama, K. 1990, PASJ, 42, 625
Bradt, H. V., Rothschild, R. E., & Swank, J. H. 1993, A&AS, 97, 355
Chu, Y.-H., Kennicutt, R. C., Jr., Schommer, R. A., & Laff, J. 1992, AJ, 103, 1545
Gallant, Y. A., & Arons, J. 1994, ApJ, 435, 230
Gotthelf, E. V. 1994, *ASCA* News, 4, 31
Gould, A. 1995, ApJ, 452, 189
Henize, K. G. 1956, ApJS, 2, 315
Jahoda, K., Swank, J. H., Giles, A. B., Stark, M. J., Strohmayer, T., Zhang, W., & Morgan, E. H. 1996, Proc. SPIE, 2808, 59
Kaspi, V. M., et al. 1997, ApJ, 485, 820
Lyne, A. G., & Graham-Smith, F. 1990, Pulsar Astronomy (Cambridge: Cambridge Univ. Press)
Ögelman, H. 1995, in ASP Conf. Ser. 72, Aspen Winter Conf. on Astrophys., Millisecond Pulsars—A Decade of Surprise, ed. A. A. Fruchter, M. Tavani, & D. C. Backer (San Francisco: ASP), 309
Rots, A. H., et al. 1998, ApJ, in press
Saito, Y., et al. 1997, *ASCA* News, 5, 34
Seward, F. D. 1989, Space Sci. Rev., 49, 385
Shapiro, S. L., & Teukolsky, S. A. 1983, Black Holes, White Dwarfs, and Neutron Stars (New York: Wiley)
Tanaka, Y., Inoue, H., & Holt, S. S. 1994, PASJ, 46, L37
Wang, Q. D., & Gotthelf, E. V. 1998, ApJ, 494, 623